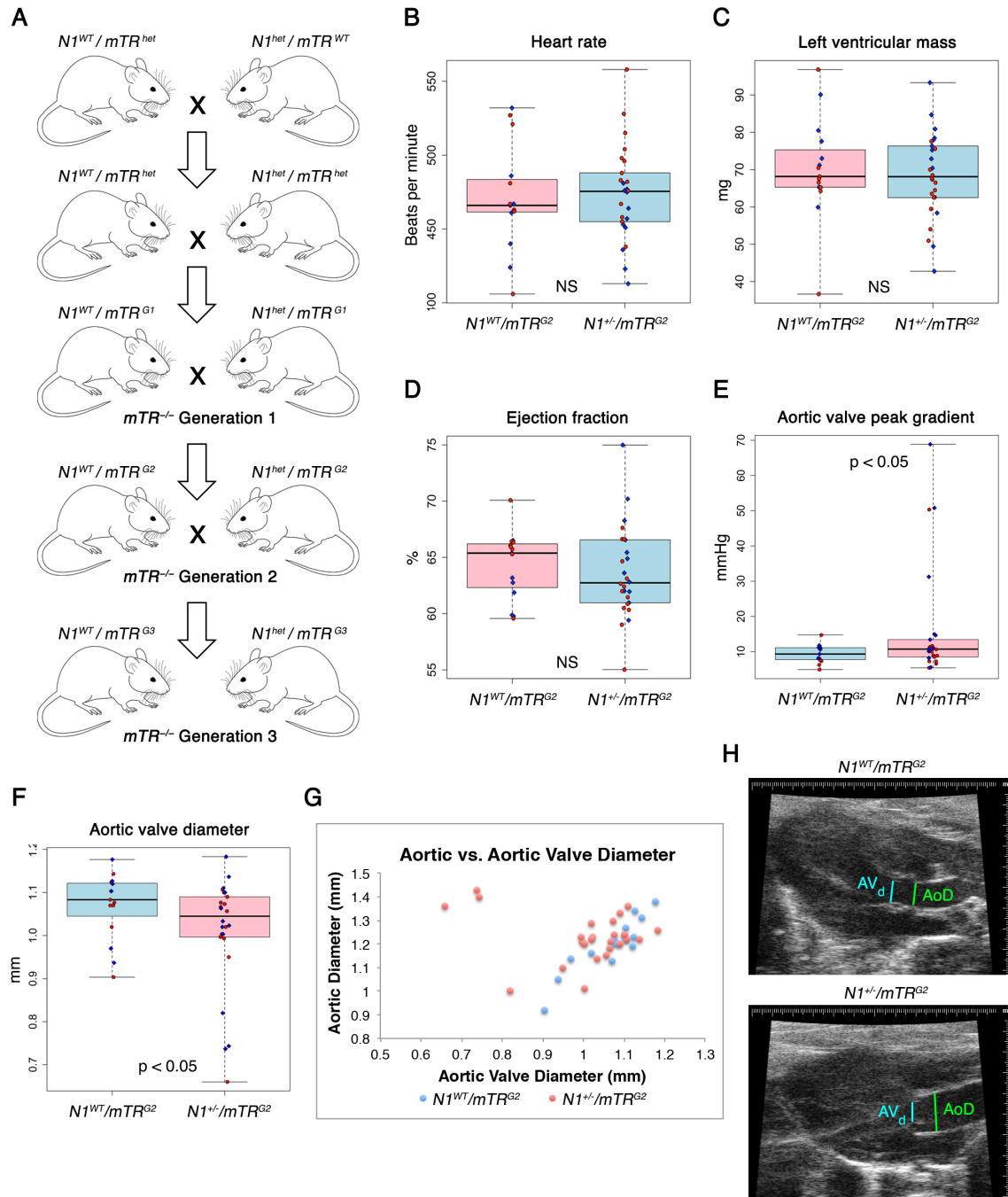


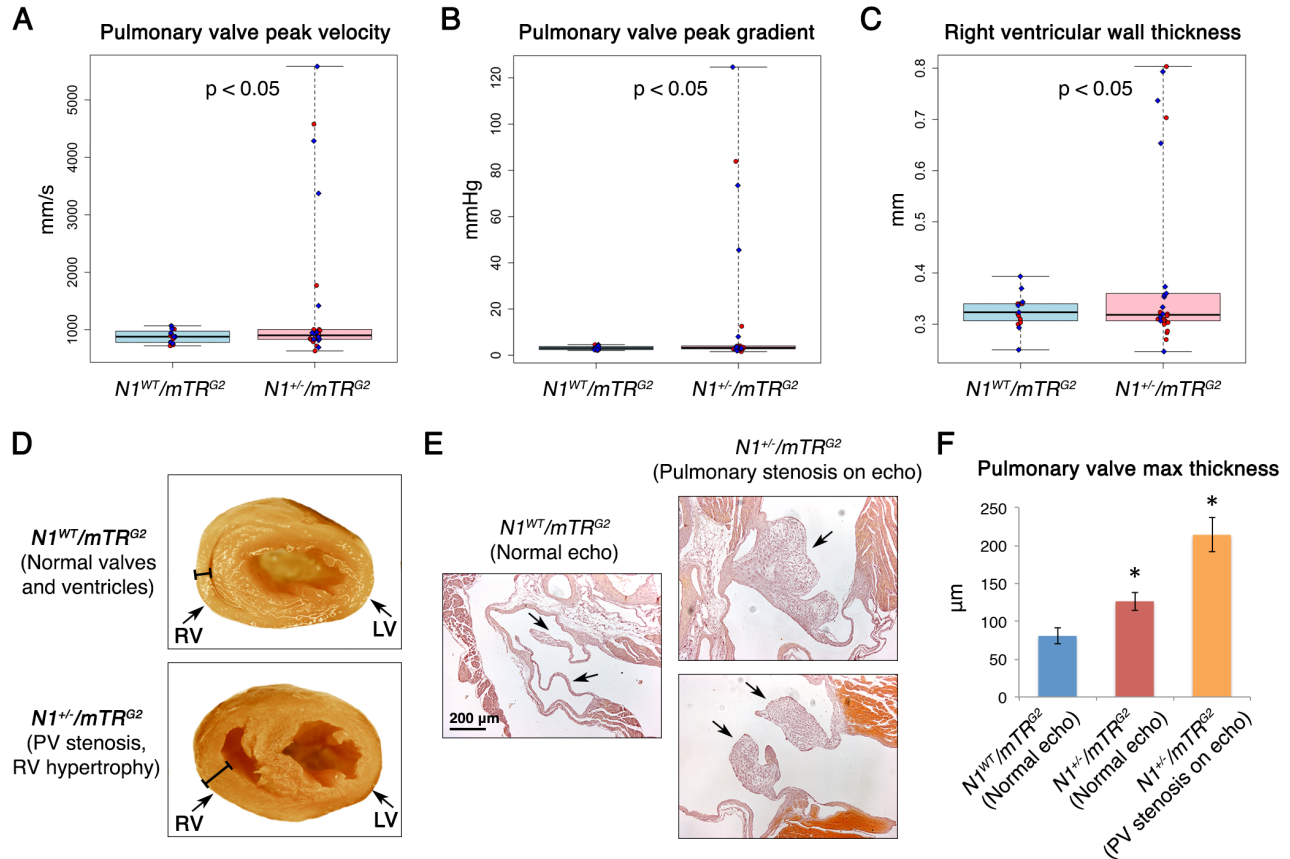
Supplemental Figure 1: Greater AV annulus narrowing is associated with ascending aorta dilation.

(A) Breeding scheme to generate $N1^{+/-}$ and $N1^{WT}$ mice that are mTR heterozygous or homozygous knockouts over successive generations. Telomere length shortens with each mTR homozygous knockout generation. $mTR^{-/-}$ generations 1, 2, and 3 are annotated as $G1$, $G2$, and $G3$, respectively. **(B)** Heart rate, **(C)** left ventricular wall thickness, **(D)** ejection fraction, **(E)** AV peak gradient, and **(F)** AV annulus diameter by echocardiography. Boxes=IQR, whiskers=range, line=median. Red=female, blue=male. NS=non-significant, $p > 0.05$ by one-sided t-test. $*p < 0.05$ by one-sided t-test. **(G)** Mice with the most narrowed AV annulus diameters had disproportionately increased ascending aortic diameters, recapitulating the clinical phenotype of aortic dilatation often associated with AV disease. **(H)** Echocardiogram of a representative $N1^{WT}/mTR^{G2}$ mouse with normal AV annulus diameter (AV_d) and aortic diameter (AoD) (top) and $N1^{+/-}/mTR^{G2}$ mouse with AS and aortic dilatation (bottom). In (B-H): $N1^{WT}/mTR^{G2}$ n=15, $N1^{+/-}/mTR^{G2}$ n=26.



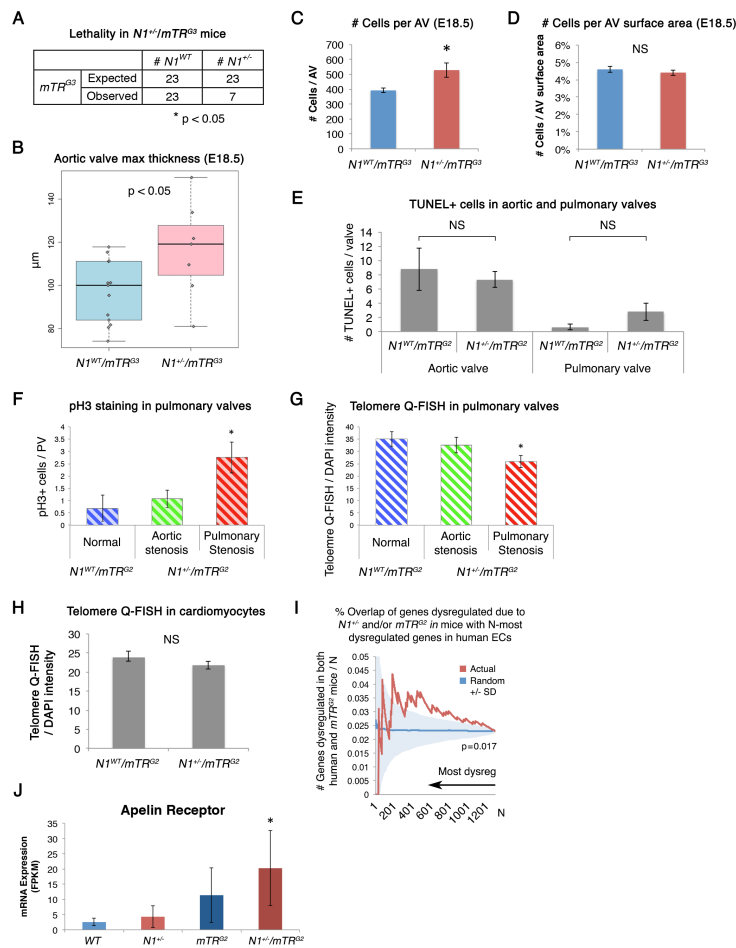
Supplemental Figure 2: Telomere shortening elicits age-dependent PS in $N1^{+/-}$ mice.

(A) PV peak velocity by echocardiography. **(B)** PV peak gradient by echocardiography. **(C)** RV wall thickness by echocardiography. **(D)** Representative cross-section of heart from $N1^{WT}/mTR^{G2}$ mouse with normal echocardiogram (n=15) or $N1^{+/-}/mTR^{G2}$ mouse with PS by echocardiography (n=4). RV and left ventricle (LV) are labeled by arrows, and RV wall thickness is labeled by brackets. **(E)** PV leaflet thickening in $N1^{+/-}/mTR^{G2}$ mice with PS by echocardiography (100% PVs showed thickening: n=4). Arrows indicate PV leaflets. **(F)** Mean PV leaflet maximum thickness ($N1^{WT}/mTR^{G2}$ with normal echo: n=12, $N1^{+/-}/mTR^{G2}$ with normal echo: n=15, $N1^{+/-}/mTR^{G2}$ with PS by echo: n=4). Errors bars=SE. In (A–C): $N1^{WT}/mTR^{G2}$ n=15, $N1^{+/-}/mTR^{G2}$ n=26. Boxes=IQR, whiskers=range, line=median. Red=female, blue=male. *p<0.05 by one-sided t-test. In (F): *p<0.05 by one-sided t-test with Benjamini-Hochberg correction.



Supplemental Figure 3: Characterization of valve leaflets and lethality in $N1^{+/-}/mTR$ mutant mice.

(A) Expected vs. observed number of $N1^{+/-}/mTR^{G3}$ compared to $N1^{WT}/mTR^{G3}$ mice at weaning age suggested 70% lethality. * $p < 0.05$ by χ^2 test. **(B)** AV leaflet maximum thickness in E18.5 embryos ($N1^{WT}/mTR^{G3}$: n=13, $N1^{+/-}/mTR^{G3}$: n=7). Boxes=IQR, whiskers=range, line=median. Red=female, blue=male. * $p < 0.05$ by one-sided t-test. **(C)** Increased cellularity in AVs of $N1^{+/-}/mTR^{G3}$ (n=8) vs. $N1^{WT}/mTR^{G3}$ (n=13) E18.5 embryos. * $p < 0.05$ by one-sided t-test. **(D)** Cell density in AVs of $N1^{+/-}/mTR^{G3}$ (n=8) vs. $N1^{WT}/mTR^{G3}$ (n=13) E18.5 embryos. **(E)** TUNEL staining showed no significant difference in apoptosis in valves of $N1^{+/-}/mTR^{G2}$ (n=14) vs. $N1^{WT}/mTR^{G2}$ (n=4) mice. **(F)** Quantification of pH3 staining for proliferation in adult $N1^{WT}/mTR^{G2}$ (n=4) and $N1^{+/-}/mTR^{G2}$ (AS by echocardiography n=5, PS by echocardiography n=5) PVs. * $p < 0.05$ by one-sided t-test with Benjamini-Hochberg correction. **(G)** Quantification of telomere Q-FISH staining for telomere length in adult $N1^{WT}/mTR^{G2}$ (hearts=3, nuclei=86) and $N1^{+/-}/mTR^{G2}$ (AS by echocardiography hearts=3, nuclei=95; PS by echocardiography hearts=2, nuclei=60) PVs. * $p < 0.05$ by one-sided t-test comparing individual nuclei. **(H)** Quantification of telomere Q-FISH staining showed no difference in cardiomyocyte telomere length in adult $N1^{+/-}/mTR^{G2}$ (hearts=5, nuclei=210) vs. $N1^{WT}/mTR^{G2}$ hearts (hearts=3, nuclei=122). **(I)** Percentage of N-most dysregulated genes in human $N1^{+/-}$ iPSC-derived ECs (5) that overlap with genes dysregulated due to $N1^{+/-}$ and/or mTR^{G2} in mice. Percentage overlap increases with greater dysregulation levels in human gene set. $P = 0.017$ by mean rank test for genes ordered by dysregulation level (red) vs. bootstrapped distribution of genes ordered randomly (1000 permutations) (blue). SD=standard deviation. **(J)** Mean mRNA expression of the *Apelin* receptor in WT (n=4), $N1^{+/-}$ (n=4), mTR^{G2} (n=3), or $N1^{+/-}/mTR^{G2}$ (n=4) AVs. Errors bars=SE. *Significant by negative binomial test with false discovery rate (FDR) correction of 10%. In (D–E, H): NS=non-significant, $p > 0.05$ by one-sided t-test. In (C–H, J): Bars=mean; error bars=SE.



Supplemental Table 1: Genes dysregulated due to mTR^{G2} and/or $N1^{+/-}$.

mRNA expression by RNA-seq of significantly dysregulated genes. See also Figure 3.

Supplemental Table 2: Gene ontology (GO) terms overrepresented in genes dysregulated due to mTR^{G2} and/or $N1^{+/-}$.

GO terms overrepresented in genes dysregulated due to mTR^{G2} and/or $N1^{+/-}$ by RNA-seq. See also Figure 3.

Movie 1: $N1^{WT}/mTR^{G2}$ echocardiogram.

Parasternal long axis view echocardiogram of $N1^{WT}/mTR^{G2}$ mouse with normal AV function.

Movie 2: $N1^{+/-}/mTR^{G2}$ echocardiogram.

Parasternal long axis view echocardiogram of $N1^{+/-}/mTR^{G2}$ mouse with thickened, calcified AV leaflets and AS and regurgitation.

Supplemental Methods

Mouse lines and echocardiography

N1^{+/-} and *mTR^{het}* C57Bl6 mice (purchased from Jackson Labs: #002797 and #004132, respectively) were used to generate double mutant animals. Power calculations (inference for independent means, $\alpha=0.05$, $1-\beta=0.80$) were completed in advance to determine appropriate sample size. All echocardiographic and histologic phenotyping was performed in a double-blinded fashion. Two animals (one *N1^{WT}*, one *N1^{+/-}*) were found to have renal cysts during echocardiography and were excluded prior to analysis due to potential for confounding effects. All analyses were performed on male and female mice at two months of age unless otherwise indicated as embryonic day 18.5 (E18.5) or neonatal (postnatal day two).

Echocardiography was performed under isoflurane anesthesia with standard measurement techniques (Supplemental Reference 1) using the Vevo 770 Imaging System (VisualSonics) equipped with an RMV-707B transducer with central frequency of 30 MHz. Peak blood flow velocity through AVs and PVs was obtained by pulsed wave Doppler in the modified parasternal long and short axis views. RV dimension and wall thickness and AV and aortic diameter were measured in the modified parasternal long axis view. The average of three cardiac cycles was used for each measurement. Stenosis (AS or PS) is defined as greater peak blood flow velocity through the given valve than any *N1^{WT}* mouse from any *mTR* generation.

Aortic root sectioning and staining

Hearts were fixed by perfusion fixation under anesthesia using isoflurane by ventricular KCl injection followed by PBS wash and fixation with 4% paraformaldehyde. Hearts were then incubated in 10% formalin overnight. The cardiac apex was cut parallel to the aortic root, and the heart tissue was then paraffin processed using standard protocols and embedded with the cut surface down. The resulting paraffin block was trimmed and angled to obtain a full three-leaflet view of the aortic root. The root was serially sectioned at 5 μm intervals from the base of the aortic sinus and mounted on slides. The slides were then deparaffinized as previously described (16) and stained with either H&E and Alizarin Red for calcification or immunohistochemical stains for Runx2 and pH3. H&E staining was performed as previously described (16) and calcification was stained with 2% Alizarin Red (pH 4.1-4.3) for 90 seconds followed by blotting and dehydrating in acetone for 20 dips, 50% acetone / 50% xylene for 20

dips, and 95% alcohol for 5 dips followed by 3 changes of 1 min in xylene and mounting in DPX. Immunohistochemical staining on deparaffinized sections was performed as previously described (16) using Abcam antibody #23981 for Runx2 and Millipore antibody #06-570 for pH3. Valve thickness was quantified using Leica software by measuring the maximum leaflet thickness in sections where leaflets were visible in the coronal plane extending into the lumen (as in the left photo in Supplemental Figure 2E). Thick AV in $N1^{+/-}$ mice is defined as thicker than any $N1^{WT}$ AV from the corresponding $mTR^{-/-}$ generation and embryonic timepoint (i.e. in Figure 2B, E18.5 $N1^{+/-}/mTR^{G3}$ thick AVs are thicker than any $N1^{WT}/mTR^{G3}$ E18.5 AV).

Telomere Q-FISH

Telomere Q-FISH on aortic root sections was performed as previously described (1–2). Briefly, paraffin sections were stained with a PNA FISH probe targeting telomeres (PNA Bio TelC-Cy3 F1002), α -smooth muscle actin antibody at 1:100 (Abcam 32575) or a cardiac Troponin T antibody at 1:100 (Abcam 74275), and Alexa Fluor 488 secondary antibody (Molecular Probes A11034). The intensity sum of all Cy3 telomere pixels vs. DAPI pixels for each nucleus in AV and PVs were then measured, and nuclei were compared from each condition as replicates using one-sided t-test ($N1^{WT}/mTR^{G2}$: hearts=3, AV nuclei=98, PV nuclei=86; $N1^{+/-}/mTR^{G2}$ with AS by echocardiography: hearts=3, AV nuclei=117, PV nuclei=95; $N1^{+/-}/mTR^{G2}$ with PS by echocardiography: hearts=2, AV nuclei=78, PV nuclei=60). Investigators were blinded during experiments, imaging, and analysis.

AV RNA-seq and analysis pipeline

Hearts were washed with PBS, and three AV leaflets were harvested by micro-dissection from each of four $N1^{WT}/mTR^{WT}$, four $N1^{+/-}/mTR^{WT}$, three $N1^{WT}/mTR^{G2}$, and four $N1^{+/-}/mTR^{G2}$ mice. Leaflets were incubated in collagenase for 20 minutes at 37 °C to dissociate cells, and RNA was isolated using the Qiagen RNeasy Micro Kit. RNA-seq libraries were constructed, sequenced, and analyzed as previously described (16) with alignment to the mm9 (*Mus musculus* assembly July 2007) genome and transcriptome and significance threshold of 10% FDR. One control sample was excluded prior to gene analysis due to high systematic noise not observed in any other sample. Data are deposited on Gene Expression Omnibus (#GSE83963).

Hi-C analysis pipeline

HUVEC contact matrices of KR-normalized interaction scores for each pairwise 25kb genomic bin were collected from Rao et al. 2014 (25), and transcriptional start sites (TSS) of each gene in the human genome were annotated with the maximum contact with a telomere. Telomere-contacting promoters were defined as any TSS with a maximum contact with telomere > 0. Mouse:human ortholog annotations were obtained from Ensembl (mm9:hg19), and the enrichment of telomere-contacting promoters for the gene groups in Figure 3F were compared to the background of all genes by the hypergeometric test with Benjamini-Hochberg correction. The group of all genes expressed in AVs refers to genes with expression >1 fragment per kilobase per million in $N1^{WT}/mTR^{WT}$, $N1^{+/-}/mTR^{WT}$, $N1^{WT}/mTR^{G2}$, or $N1^{+/-}/mTR^{G2}$ mice.

Statistics

Comparison of independent, continuous variables (e.g. quantification of echocardiography, valve thickness and cellularity, pH3 staining for proliferation, TUNEL staining for apoptosis, telomere Q-FISH staining) was conducted by one-sided t-test with significance threshold $p < 0.05$ with Benjamini-Hochberg correction for multiple hypothesis testing. Comparison of independent, categorical variables was conducted by X^2 test (e.g. quantification of Alizarin red staining for calcification, lethality, overlap of gene sets) or Barnard's test (e.g. age-dependent disease progression) with significance threshold $p < 0.05$. Comparison of fold enrichment of telomere-contacting promoters by gene group was conducted by hypergeometric test with Benjamini-Hochberg correction with significance threshold $p < 0.05$. Comparison of overlap between human and murine genes dysregulated by N1 haploinsufficiency by dysregulation level was conducted by mean rank test for genes ordered by dysregulation level versus a bootstrapped distribution of genes ordered randomly (1000 permutations) with significance threshold $p < 0.05$. Analysis of RNA-seq differential expression was conducted by negative binomial test with FDR correction of 10% using USeq (Supplemental Reference 2). In Figure 2 and Supplemental Figure 3, lethality is the number of fewer $N1^{+/-}$ mice observed than expected based on the number of $N1^{WT}$ mice at the given generation.

Supplemental References

1. Rottman JN, et al. Echocardiographic evaluation of ventricular function in mice. *Echocardiography*. 2007;24(1):83–89.
2. Nix DA, et al. Empirical methods for controlling false positives and estimating confidence in CHIP-Seq peaks. *BMC Bioinformatics*. 2008;9:523.